Lateralization of comodulated complex waveforms

Kourosh Saberi[a)]

Psychoacoustics Laboratory, Department of Psychology, University of Florida, Gainesville, Florida 32611

(Received 13 September 1994; revised 23 May 1995; accepted 2 June 1995)

This study examines the ability to lateralize a complex signal characterized by correlated temporal activity across widely separated frequency regions. The high-frequency complex consisted of two narrow-band stimuli. The two stimuli had common interaural delays but different carriers centered on nonoverlapping critical bands. Two basic conditions were examined: The narrow-band stimuli had temporal envelopes which were (1) identical or (2) different. In the first experiment, narrow bands of *noise* were used which either had identical temporal envelopes (comodulated) or statistically independent envelopes (CFs=2550 and 3350 Hz). In the second experiment, two sinusoidally amplitude-modulated (SAM) tones were used whose modulators either had the same starting phase or a different starting phase (CFs=2550 and 4000 Hz). Results of the first experiment showed that for bandwidths narrower than 300 Hz, comodulated bands produced significantly lower interaural-delay thresholds compared to independent bands. Results of the second experiment showed that when the two SAM tones (100-Hz modulation rate) had the same modulator starting phase, interaural-delay thresholds were lowest.

PACS numbers: 43.66.Pn

INTRODUCTION

Contrary to predictions of *critical band theory*, signal detection in one auditory filter may be affected by activity in other filters. When steady-state stimuli are used, observers may use information derived from the profile of the spectrum to detect increments or decrements in the amplitude of a single component of a multitone complex (Spiegel and Green, 1982; Green *et al.*, 1983; Green, 1988; Green *et al.*, 1995). When time-varying signals are used, the coherence of temporal envelopes of sounds in remote filters may facilitate or impair the detectability of a signal within one of these filters (Hall *et al.*, 1984; Hall, 1986; Hall and Grose, 1991; McFadden, 1987; Cohen and Schubert, 1987a, b, 1991; Richards, 1987; Yost and Sheft, 1989; Grose and Hall, 1992). Such phenomena have collectively been referred to as across-frequency effects (see Moore, 1990 for a review).

Similar and seemingly related findings have been reported in the sound-localization literature. It has, for example, been suggested that the spectral profile of broadband stimuli, particularly stimuli with energy above 5 kHz, may be the basis for estimating the vertical position of sound sources (Batteau, 1967; Butler and Belendiuk, 1977; Shaw, 1979; Kuhn, 1987). Lateralization studies have shown across-frequency effects in the form of interference with the detectability of interaural differences (McFadden and Pasanen, 1976; Zurek, 1985; Buell and Hafter, 1991; Buell and Trahiotis, 1993; Buell and Trahiotis, 1994; Trahiotis and Bernstein, 1990; Dye, 1990; Stellmack and Dye, 1993). In these latter studies, two or more narrow-band stimuli with different interaural differences and carriers are usually used. A typical report is that the detectability of an interaural difference in one narrow-band stimulus may be degraded in the presence of other stimuli which have different interaural values, even though the signal and interfering stimuli contain very different spectral energies.

The aim of this study is to examine across-frequency effects on the lateralization of complex sounds whose time-varying envelopes are correlated across frequency regions; these sounds are referred to as comodulated sounds in reference to similar stimuli used in intensity-detection tasks. There are three studies which have examined changes in lateralization thresholds by temporally comodulating sounds in different frequency channels. Heller and Richards (1990), and Heller and Trahiotis (1995) have reported on the detectability of an interaural time or level difference (ITD or ILD) in a target, high-frequency narrow-band sound in the presence of an *interfering* sound at a remote frequency region. The two sounds were either temporally comodulated or independent. The comodulated and independent conditions produced nearly identical thresholds, suggesting that binaural interference did not depend on comodulation across frequencies. Stellmack (1992), however, using *low-frequency* narrow bands of noise reported that binaural interference did, in some conditions, increase when narrow-band signals were comodulated.

The current study, unlike studies of interference, is concerned with the ability of observers to combine, constructively, binaural information across frequency regions. There is both psychophysical (Dye, 1990; Buell and Trahiotis, 1993; Trahiotis and Stern, 1994; Stern *et al.*, 1988) and physiological (Takahashi and Konishi, 1986) evidence that such information from sounds with different spectral contents but common interaural delays may be effectively combined. There are also many naturally occurring signals which have consistent temporal-envelope activity *and* common interaural differences across broad frequency regions. Speech signals, for example, have envelope fluctuations which are highly correlated across frequencies (Houtgast and van den Brink, 1990; Hall and Haggard, 1983; Festen and Plomp,

[a)]Current address: 36-767, Research Laboratory of Electronics, Massachusetts Institute of Technology, Cambridge, MA 02139.

1990; Grose and Hall, 1992). An improvement in the ability to process binaural information in such signals compared with sounds which are not temporally synchronous across frequency may facilitate their localization and detection in acoustically complex fields.

In the first of two experiments reported here, the high-frequency signal consisted of two narrow bands of noise with different center frequencies, but common interaural delays. In the second experiment, sinusoidally amplitude-modulated (SAM) tones were used; these signals have periodic and regular envelope fluctuations as compared to the irregular envelopes of noise bands. In this latter experiment, the complex consisted of two SAM tones with different carriers, but again, with common interaural delays. As reported in later sections, when signals were comodulated at rates below about 200 Hz, ITD thresholds were lower than those obtained for sounds that were not comodulated.

I. EXPERIMENT I: LATERALIZATION OF A STIMULUS CONSISTING OF TWO COMODULATED NARROW BANDS OF NOISE WITH COMMON ITDs

A. Procedure

On each trial of a two-interval, forced-choice task (2IFC), two dichotic noise bursts were presented. The two bursts were separated by 300 ms. The noise bursts carried equal-magnitude interaural delays; however, for one noise burst, the waveform led the left ear and for the other noise burst it led to the right ear. The subject's task was to identify the order of presentation of the bursts (i.e., left-leading then right or right-leading then left). Each run consisted of 100 trials. Visual feedback was provided immediately after each trial. A minimum of 400 trials was run at a minimum of two interaural delays (method of constant stimuli). A delay of zero for 50% correct detection was arbitrarily chosen as an additional point. A least-squares procedure was used to determine a 75% threshold from a fitted normal probability integral.

The noise bursts consisted of either one or two noise bands. The center frequencies of the two bands were always 2550 and 3350 Hz. The bandwidth of each noise band was 50, 100, 200, or 300 Hz. When two bands were presented simultaneously, both bands had the same bandwidth and ITD. Each band was presented for 400 ms with a 10-ms linear rise–fall ramp.

Four experimental conditions were examined. Lateralization thresholds were measured for (1) low-frequency band alone, (2) high-frequency band alone, (3) linear sum of two independent noise bands, and (4) linear sum of the two noise bands, but the noises were constructed to have a common envelope.

All signals were computed in an IBM PC. Before each 2-h experimental run, 2400 dichotic noise pairs were generated overnight and stored on hard disk. During an experimental session, subjects completed 12 100-trial runs. Throughout a given run, the bandwidth, ITD, and condition were fixed. On each trial of each run, two dichotic noise samples (one for each interval of the 2IFC) were selected without replacement and presented to the subject. Thus a given subject did not hear the same noise sample twice. Data for the 16 signal combinations (four bandwidths by four conditions) were collected using a random-without-replacement scheme between blocks where a random-number generator selected one bandwidth, one condition, and one ITD.

Signals were presented through locally constructed, digital-to-analog converters (DAC) at a sampling rate of 20 kHz and low-pass filtered at 10 kHz (Kemo, VBF-8). The spectrum level of the noise was 45 dB SPL as measured for the average of 100 samples with a spectrum analyzer (Hewlett–Packard 3582-A). Envelope delays between left and right channels were checked for accuracy with a dual-channel storage oscilloscope. These signals were then led to a single-walled steel sound booth and presented to subjects through STAX (SR-5) electrostatic headphones whose frequency responses were flat within ±3 dB between 50 and 20 000 Hz. Each of the four subjects (SH, JT, KC, KS) was practiced on the various conditions of the experiment for a minimum of 1 week, in 2-h daily sessions before data collection began. Three subjects were male and one female. All were students at the University of California. Their ages ranged from 19–31 and had normal hearing to the best of their knowledge.

B. Signal generation

Each digitally generated noise band was the sum of sinusoidal components at 2.5-Hz spacing (1/duration). The two noise bands were of the form

$$w(t)=\sum_{i=-m}^{m} a_i \cos[2\pi(f_0+\delta_i)t+\Theta_i], \tag{1a}$$

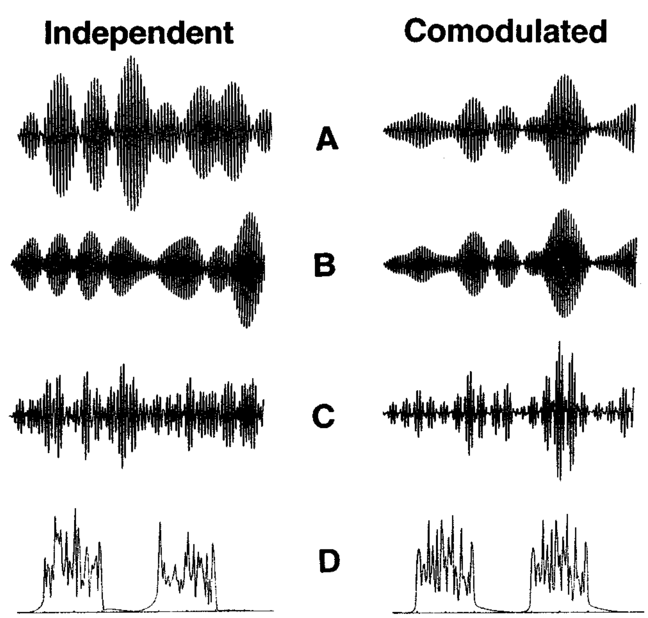

FIG. 1. Left traces show the waveforms and spectra used for condition 3 (independent) and right traces for condition 4 (comodulated). Traces A and B show time waveforms of the lower- and higher-carrier noise bands, trace C shows the sum of A and B, and trace D shows the spectrum of C.

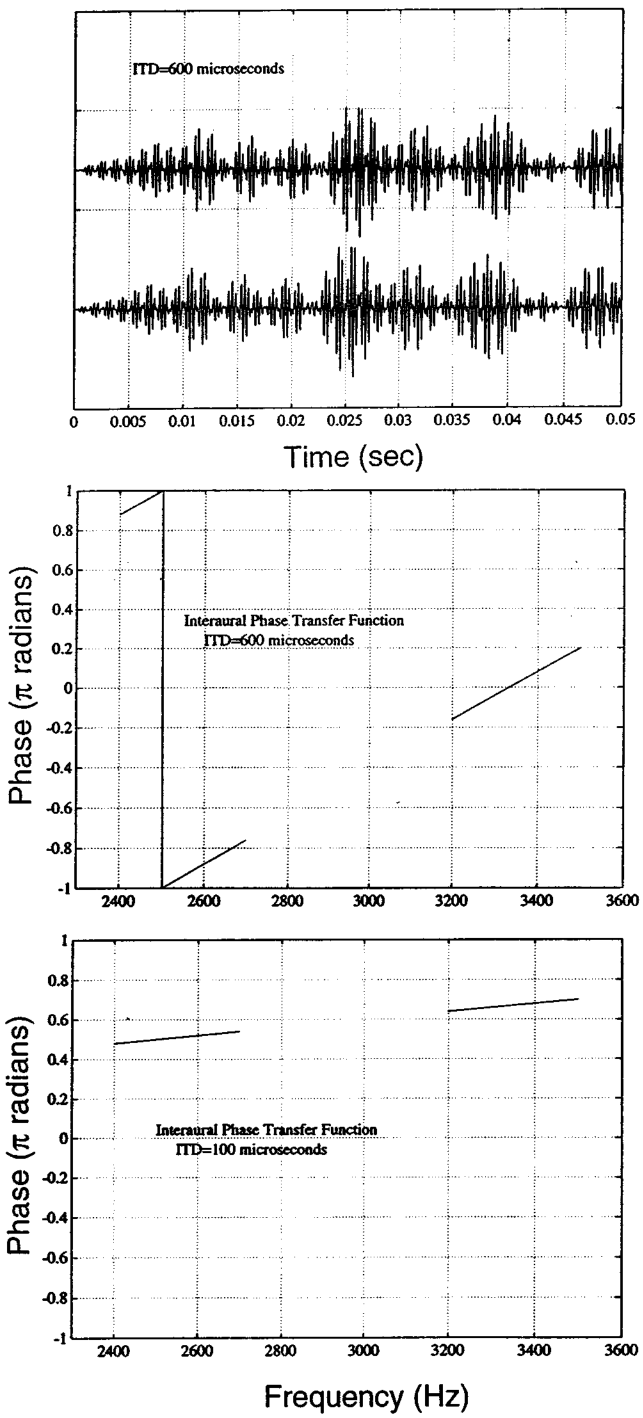

FIG. 2. The top panel shows two waveforms, each composed of two comodulated 300-Hz-wide noise bands with different carriers. The upper waveform is delayed by 600 μs relative to the lower waveform via a linear-phase-shift algorithm. One waveform is presented to the left ear, and the other to the right ear. The slope (b) of the phase transfer function, shown in the middle panel (for *two* 300-Hz bands) is a linear function of ITD. The vertical break is due to the cyclic nature of the phase shift. The lower panel shows a more shallow transfer function for an ITD of 100 μs.

$$w^*(t)=\sum_{i=-m}^{m} a_i^* \cos[2\pi(f_0+\Delta f+\delta_i)t+\Theta_i^*], \qquad (1b)$$

where δ is the separation between the frequency components added to generate each noise band (2.5 Hz), f_0 is the center frequency of the lower noise band (2550 Hz), Δf is the difference between the center frequencies of the lower- and higher-frequency noise bands (800 Hz), and $2m+1$ is the number of components constituting the noise band where $m=\mathrm{BW}/2\delta$ (for a bandwidth BW=100 Hz, $m=20$ and each 100-Hz-wide noise band consisted of 41 sinusoidal components).

The amplitude of each component was sampled from a Rayleigh distribution and the phases from a uniform $(0,2\pi)$ distribution. Each noise band, thus generated, was Gaussian with an envelope modulation rate, based on the average number of peaks per second, equivalent to 0.64 times its bandwidth (Rice, 1944).

In cases where two bands were summed $[w(t)+w^*(t)]$, the envelopes of the two bands were either independent or comodulated. If the bands were to be independent (condition 3), then the amplitude (a_i and a_i^*) and phase (Θ_i and Θ_i^*) of each component (i) of each band was determined independently. If the envelopes were comodulated (condition 4), then the amplitude and phase value determined for one component of one band were used to generate the corresponding component for the other band ($a_i=a_i^*$; $\Theta_i=\Theta_i^*$).

Figure 1 shows the time waveforms and spectra of the noise bands $[w(t)$ and $w^*(t)]$. The left and right traces are for the independent and comodulated conditions, respectively. Traces A and B show the lower- and higher-center-frequency (CF) bands, trace C their sum $[w(t)+w^*(t)]$, and trace D the spectrum of the combined waveforms (the spectrum of C). Trace C (left) shows the type of waveform used for condition 3 (independent waveform conditions) and trace C (right) shows the type of waveform used in condition 4 (comodulated).

Because lateralization thresholds were to be determined, each signal was presented to subjects dichotically. For illustration, a 50-ms segment of a waveform used for condition 4 (comodulated) is depicted in Fig. 2. The time waveform of this signal $[w(t)+w^*(t)]$ was presented to both ears. However, in order to measure lateralization thresholds, the signal to one ear (upper waveform in the top panel of Fig. 2) was delayed relative to the other (lower waveform). A linear phase-shift algorithm was used to delay the dichotic noise band to one ear. First, a band of noise was generated for one ear as described above. For the other ear, each component of the noise for the first ear was phase shifted by a value corresponding to the desired interaural delay. Thus two identical noise bands (one for each ear) were obtained with one of them delayed relative to the other. This constituted the dichotic signal for one interval of the 2IFC. For the other interval the same delay was used to generate a new dichotic noise band favoring the ear opposite to that favored in the first interval. Thus, for conditions 3 and 4, the waveforms presented to the right and left ears, respectively, for one interval of the 2IFC were of the form

$$L(t)=\sum_{i=-m}^{m} a_i \cos[2\pi(f_0+\delta_i)t+\Theta_i+\phi_{Li}] + \sum_{i=-m}^{m} a_i^* \cos[2\pi(f_0+\Delta f+\delta_i)t+\Theta_i^*+\phi_{Li}], \qquad (2a)$$

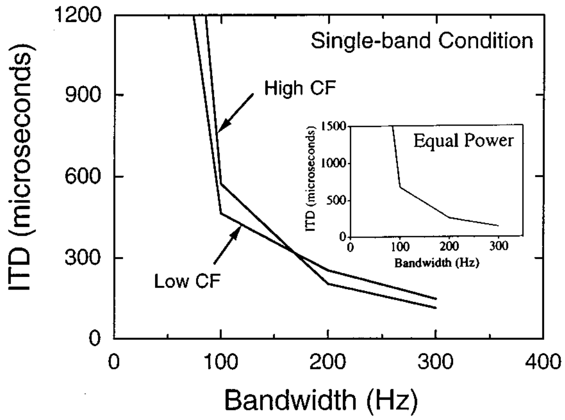

FIG. 3. ΔITD thresholds for 75% detection measured for single noise band conditions (1 and 2) as a function of bandwidth. The lines are interpolations through the averaged data for four subjects at bandwidths of 50, 100, 200, and 300 Hz. Thresholds were measured for a constant noise-power density (N_0). The inset shows that the shape of the function is unaffected when equal-power noise bands are used. The single function in the insert is the averaged thresholds for lower- and higher-CF bands measured individually.

$$R(t)=\sum_{i=-m}^{m} a_i \cos[2\pi(f_0+\delta_i)t+\Theta_i+\phi_{Ri}] + \sum_{i=-m}^{m} a_i^* \cos[2\pi(f_0+\Delta f+\delta_i)t+\Theta_i^*+\phi_{Ri}], \tag{2b}$$

where $\phi_i=2\pi \mathrm{ITD} f_i$ and ITD is interaural delay in seconds. If the right ear carried the leading waveform then $\phi_{Li}=0$ and if the left ear carried the leading waveform then $\phi_{Ri}=0$. The middle panel of Fig. 2 shows the phase transfer function between the two waveforms of the top panel (600-μs ITD). The *slope* (b) of this function determines the magnitude of ITD with larger slopes representing greater ITDs $[\phi(f)=bf$: $b=2\pi$ ITD]. For comparison, in the lower panel of Fig. 2 the phase transfer function for a 100-μs ITD is shown.[1]

C. Results

Figure 3 shows averaged data for four subjects obtained for the single-band conditions. Each line connects through four points at 50-, 100-, 200-, and 300-Hz bandwidths.[2] Each line represents the averaged performance for the four observers. No significant differences were observed in lateralization thresholds measured for individual bands centered at 2550 and 3350 Hz. As bandwidths increased, lateralization thresholds improved. Both the similarity of thresholds for different CFs and improvements in thresholds for wider bandwidth signals have been reported by Nuetzel and Hafter (1981) and Henning and Ashton (1981). An increase in bandwidth, given the same spectrum level, corresponds to increased signal energy and one might conclude that the improved thresholds reflect this increase in energy. The inset in Fig. 3 shows lateralization thresholds measured when the overall power in the different bands were adjusted to match that of the 200-Hz-wide noise band. A single carrier (high CF) was used and the level of the noise band was increased

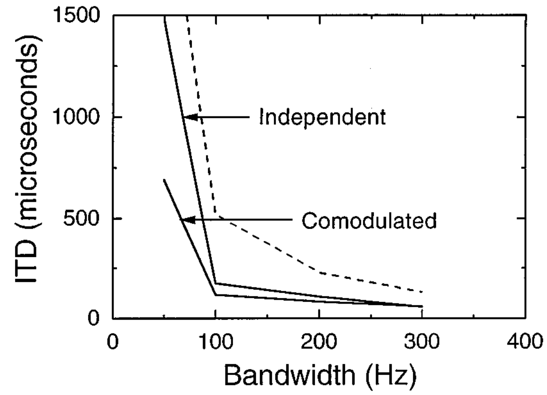

FIG. 4. The dashed line shows the average of the single-band conditions (from Fig. 3). The two solid lines show interpolation through 75% ΔITD thresholds averaged for four subjects at bandwidths of 50, 100, 200, and 300 Hz.

for the 50- and 100-Hz bands by 6 and 3 dB, respectively, and decreased for the 300-Hz noise band by 1.8 dB. All other procedures were identical to those described above. Results show that this adjustment had no noticeable effect on the shape of the functions in Fig. 3; thus improvements in lateralization are not primarily due to increased energy with bandwidth. Among possible reasons for improved thresholds with bandwidth is an increase in the modulation rate of the temporal waveform. The reader should, however, be aware that peripheral bandpass filtering may limit the effective signal bandwidth and therefore modulation rate.

Figure 4 plots averaged data for four subjects for conditions 3 (independently modulated) and 4 (comodulated). The individual datapoints have been eliminated from the figure for clarity; however, individual data for all subjects will be presented shortly as a normalized ratio (see below) in Fig. 5. For the narrower bandwidth conditions, subjects had lower ITD thresholds when the bands were comodulated. Again, thresholds improved with increasing bandwidths. Plotting data, however, from all conditions in the same figure, (4) makes the visual inspection of wider bandwidth conditions difficult because of the relatively high thresholds for the

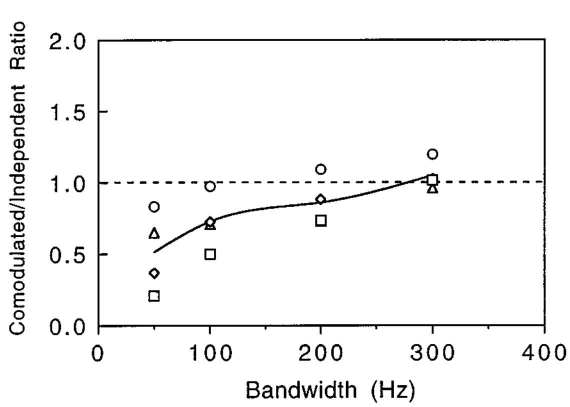

FIG. 5. The ordinate is the value of the subject's 75% threshold measured in the comodulated condition divided by threshold for independent condition (see Fig. 4). Each symbol represents data from one observer. The solid line is the average of this ratio for the four subjects. The dashed line marks unity.

50-Hz condition. The data of Fig. 4 were, therefore, replotted in Fig. 5 as a ratio of the comodulated to independent-band thresholds. If there were no differences between thresholds in the two conditions (3 and 4), one would expect all points to fall on a ratio line of unity (dashed horizontal line). Each symbol in this figure represents data for one subject. Nearly the entire data set falls below or near the dashed line. The difference, however, becomes smaller as bandwidths increase. This is not surprising. Across-frequency effects in intensity-detection problems have also been shown to decrease with increasing bandwidth and are virtually nonexistent for bandwidths wider than about 400 Hz (Schooneveldt and Moore, 1989). The results for the wider bandwidth conditions, and therefore higher modulation rates, are consistent with those reported for the interference experiments of Heller and Richards (1990) and Heller and Trahiotis (1995) in that no difference in thresholds was observed between the independent and comodulated conditions.

D. Low-frequency carriers

To further examine temporal-envelope effects on lateralization, an additional control experiment was run in which all conditions were identical to conditions 3 (independent) and 4 (comodulated), except that the CFs for the two noise bands were set at 500 and 750 Hz. Only one bandwidth was examined (50 Hz) which produced the greatest averaged departure from the ratio of 1.0 in Fig. 5. Because envelope ITD information at low frequencies is dominated by carrier ITDs (Bernstein and Trahiotis, 1985), little difference between the comodulated and independent conditions was expected. The ratio of the comodulated to independent band thresholds for four subjects (FW, SH, JT, KC) were 1.02, 0.91, 0.99, and 1.05, respectively; all are very near unity.

II. EXPERIMENT II: LATERALIZATION OF A STIMULUS CONSISTING OF TWO SAM TONES WITH COMMON ITDs

A. Procedure

The major change in the procedures for experiment II (compared to experiment I) was that an adaptive technique was used instead of the constant stimulus method. A two-down, one-up procedure was used which tracks the 70.7% correct response on the subject's psychometric function. The subject's task was the same as that in experiment I. Visual feedback was provided after each trial. The two SAM tones had different carrier frequencies, but the same ITDs, modulation rate (100 Hz), and levels. They were different only in that the starting phase of the modulation envelope for one SAM could be different than that of the other (by 0°, 30°, 60°, 90°, 120°, 150°, or 180°). Each condition was defined by the modulation-phase disparity. Each subject completed a minimum of six runs per condition. The step change in interaural delay was 0.2 log μs up to the fourth reversal and 0.05 log μs for the remaining trials. These values correspond to 4- and 1-dB step sizes for intensive continua. The starting ITD value was 1300 μs (650 μs in each interval of the 2IFC). The run continued until 12 reversals were obtained. If a reversal occurred on the first five trials it was not counted toward the total number of reversals. The first four reversals were discarded and the values of interaural delays for the remaining eight reversals were averaged to obtain one estimate of threshold.

Lateralization thresholds were measured for a complex signal consisting of two SAM tones, one centered at 2550 Hz and the other at 4000 Hz. The carriers had a zero starting phase and were not interaurally delayed.

Each SAM was 400 ms in duration with a 10-ms cosine-squared rise–fall ramp. The two SAMs were of the form

$$s(t)=[1+m\ \sin(2\pi gt)]\sin(2\pi f_0 t), \tag{3a}$$

$$s^*(t)=[1+m\ \sin(2\pi gt+\Theta_m)]\sin[2\pi(f_0+\Delta f)t], \tag{3b}$$

where m is unity, producing a modulation depth of 100%, g is the modulation frequency equal to 100 Hz, $f_0=2550$ Hz and $(f_0+\Delta f)=4000$ Hz are the carrier frequencies, and Θ_m is the parameter of the study determining the relative phase in radians of the modulation envelopes between waveforms $s(t)$ and $s^*(t)$. Each SAM was never presented alone, but in the form of the complex

$$S(t)=s(t)+s^*(t). \tag{4}$$

Each complex was presented dichotically. To measure lateralization thresholds, the modulation phase of each SAM was shifted an additional amount $\phi=2\pi\mathrm{ITD}g$ which corresponded to the desired ITD in seconds. Thus the entire waveforms presented to the left and right ears, respectively, were of the form

$$L(t)=[1+m\ \sin(2\pi gt+\phi_L)]\sin(2\pi f_0 t)+[1 \\ +m\ \sin(2\pi gt+\Theta_m+\phi_L)]\sin[2\pi(f_0+\Delta f)t], \tag{5a}$$

$$R(t)=[1+m\ \sin(2\pi gt+\phi_R)]\sin(2\pi f_0 t)+[1 \\ +m\ \sin(2\pi gt+\Theta_m+\phi_R)]\sin[2\pi(f_0+\Delta f)t]. \tag{5b}$$

If the right ear was to lead the left, then $\phi_L=0$ and if the left ear was to lead the right, then $\phi_R=0$.

The top, middle, and lower panels of Fig. 6, respectively, show 0°, 90°, and 180° phase disparity between the modulation envelopes of $s(t)$ and $s^*(t)$. The top two waveforms in each panel show the waveform of each SAM $[s(t)$ and $s^*(t)]$, and the bottom trace in each panel shows their sum $S(t)$. The ratio of the peak-to-valley amplitudes of the envelope of the summed waveform decreases with increasing modulator phase shift. We will return to this point in Sec. III.

All signals were computed before each trial of the adaptive procedure using an IBM PC and an array processor [Tucker–Davis Technologies (TDT) AP2]. Data for the seven phase conditions (Θ_m) were collected in random order. During the 60 trials of a single experimental run, only one phase condition was examined. Signals were presented through 16-bit digital-to-analog converters (TDT DA2) at a sampling rate of 20 kHz and were low-pass filtered at 10 kHz. The sound-pressure level for a continuous SAM-tone complex was 60 dB. Continuous Gaussian noise, low-pass

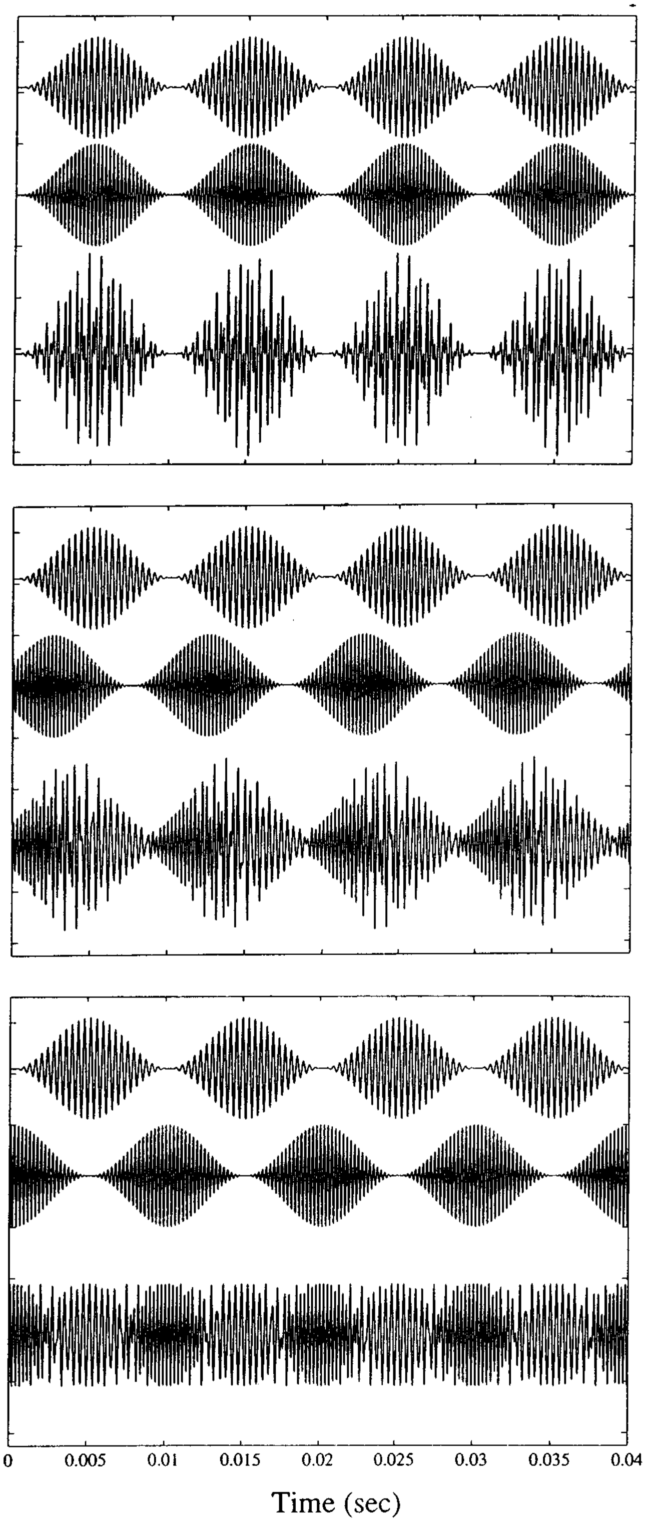

FIG. 6. The type of stimuli used in experiment II. Each panel shows two SAMs (top two waveforms in each panel) with the same modulation rate (100 Hz) but different carriers (2.55 and 4.0 kHz). The lower trace in each panel shows the sum of the top two traces within that panel. The top panel shows the two SAMs when the starting phase of their modulators were the same, the middle panel when one was phase shifted by 90°, and the lower panel when one was phase shifted by 180°.

filtered at 1.5 kHz, was presented at a spectrum level of 32 dB SPL as background to mask low-frequency intermodulation distortions (Henning, 1974; 1980; Nuetzel and Hafter, 1981). Envelope delays between left and right channels (interaural delays ϕ) were checked for accuracy with a Philips dual-channel storage oscilloscope (model PM 3335). These signals were led to a single-walled sound booth and presented to subjects through Sennheiser (HD-450) headphones. Each of the three subjects (JM, YB, LF) was practiced on various conditions of the experiment for a minimum of 6 h before data collection began. All subjects had previous experience in lateralization experiments. Two subjects were female and one male and their ages ranged from 18–23. All were students at the University of Florida and had normal hearing within 10 dB of ISO standards for frequencies between 125 and 8000 Hz as determined by a Bekesy audiometer.

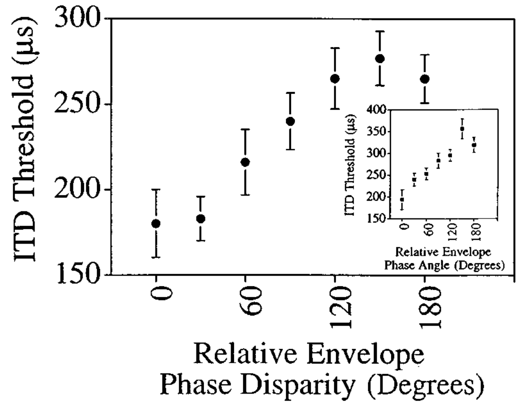

FIG. 7. Average results for three subjects from experiment II. The inset shows data collected for the same conditions and stimuli, except that the signal level was lowered to 30 dB SPL.

B. Results

Figure 7 shows averaged results. Error bars are one standard error of the mean. Consistent with results of experiment I, lowest ITD thresholds are observed when the SAMs are modulated in phase (0° condition). Thresholds increase as the envelopes are increasingly phase shifted. In a control condition, experiment II was repeated without the low-pass masking noise, but with SAM tones whose sound-pressure levels were reduced to 30 dB SPL. These low levels were used to reduce leakage through common frequency channels. The results of this control condition, shown in the inset to Fig. 7, are similar to those in Fig. 7, except that the thresholds are higher because the signal SPLs were lower.

III. DISCUSSION

A. Combining interaural information from individual bands

Assuming that the noise which limits the detectability of ITDs is a Gaussian process with mean ITD and standard deviation σ_I, improvements in discrimination for combined conditions may be predicted from thresholds for individual bands. In a 2IFC task, the $\sigma = \sigma_I/\sqrt{2}$ for each band is estimated as the value of ΔITD at threshold divided by 0.95 (d' for 75% detection). Because in the combined conditions (3 and 4), by definition, $\mathrm{ITD}_C = \mathrm{ITD}_L = \mathrm{ITD}_H$ (where

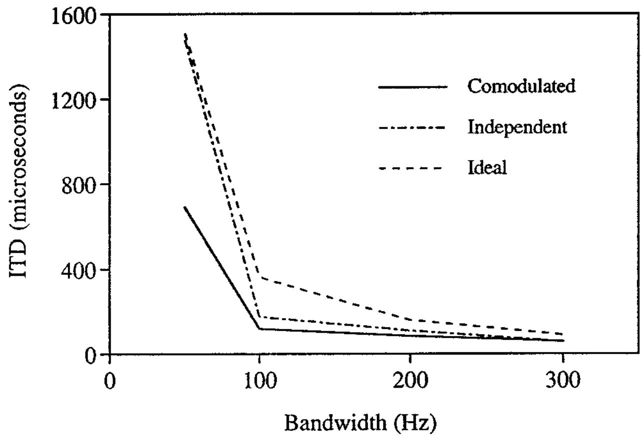

FIG. 8. The upper and lower solid lines are averaged data for the comodulated and independent noise band conditions (3 and 4) of experiment I, respectively. The dashed line is ideal predictions based on Eq. (7).

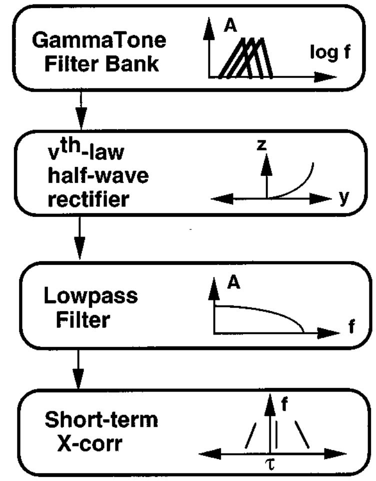

FIG. 9. A schematic of the cross-correlation model.

C=combined, L=low, H=high frequencies), Eq. (6) may be derived from the vector rule (Green and Swets, 1966, pp. 271–275):

$$\sigma_C = \frac{\sigma_L \sigma_H}{\sqrt{\sigma_L^2 + \sigma_H^2}}. \tag{6}$$

Performance for ideal detection is then

$$\mathrm{ITD}_C = d' \sigma_C. \tag{7}$$

This simple model has been applied to studies of interference in which multicomponent sounds with unequal ITDs have been used. In some, but not all, cases the model is a good predictor of observer performance (Buell and Hafter, 1991; Buell and Trahiotis, 1993). In other studies (Heller and Trahiotis, 1995), subjects outperform the ideal. Figure 8 shows averaged thresholds for four subjects replotted from Fig. 4 of the current paper. The dashed line shows predictions of Eq. (7). As with the Heller and Trahiotis study, subjects performed better than ideal for both combined conditions, though at least for the 50-Hz bandwidth case, ideal and independent conditions produce similar values. It seems, therefore, that for most cases additional information is available to observers. One possible source is "straightness" information across frequency associated with the putative cross-correlator output. The two noise bands do not simply generate "twice" the activity in the cross spectrum, but the presence of peaks at common delays across frequency regions provides information about the trajectory of these peaks (Stern *et al.*, 1988), speculated to be important in lateralization.

B. A short-term cross correlation

ITD thresholds obtained for comodulated bands were smaller than those measured for independent bands. Consistent with these results is an analysis based on short-term cross correlation. Assume that the binaural system crosscorrelates the input stimulus, for example the SAM complex in experiment II, with a time constant of 5 ms. If the SAMs constituting the complex have modulation envelopes that are in phase (see Fig. 6), then the waveform peaks for individual SAMs will occur simultaneously in one 5-ms period, and the waveform dips in the next 5-ms period (because the SAMs have a modulation rate of 100 Hz). If the SAM envelopes are out of phase, then each 5-ms period will carry the peak from one SAM and the dip from the other. The *simultaneity of peaks* in the complex SAM will generate activity in the short-term cross-correlation plane which allows an estimation of the straightness of trajectories of cross-correlation peaks across frequency. When the SAMs are out of phase, however, this straightness measure is substantially weaker. This straightness measure has been used in the weighted-image model of Stern *et al.* (1988) to model lateral position estimates of complex binaural stimuli. It can be shown, with few simple assumptions, that straightness contributes to improved *discrimination* of interaural delays for the type of stimuli used in the current study.[3]

A schematic diagram of a short-term cross-correlation model used in the current analysis is shown in Fig. 9. The GammaTone filter bank (Holdsworth *et al.*, 1988) consisted of 30 logarithmically spaced filters from 2 to about 5 kHz ($\mathrm{CF}_{(i+1)} = 1.032\ \mathrm{CF}_i$). The impulse response of this filter is

$$g(t) = t^3 e^{-2\pi bt} \cos(2\pi f_0 t + \phi), \tag{8}$$

where b in Hz controls the duration of the impulse response; f_0 and ϕ are the carrier frequency and phase, respectively. This function has the form of an amplitude-modulated carrier with an envelope proportional to a fourth-order Gamma density function, hence the term GammaTone. The frequency response of the filters may be derived directly from the Fourier transform of $g(t)$:

$$G(t) \propto \left[1 + \frac{j(f-f_0)}{b}\right]^{-4} + \left[1 + \frac{j(f+f_0)}{b}\right]^{-4}$$
$$(-\infty < f < \infty). \tag{9}$$

The output of this filter bank was followed by νth-law, half-wave rectification (ν=3):

$$R_\nu[z] = \begin{cases} z^\nu, & \text{for } z \geqslant 0, \\ 0, & \text{for } z \leqslant 0, \end{cases} \tag{10}$$

and a low-pass filter with an 800-Hz cutoff. Such a circuitry has several desirable properties. The νth-law rectifier (Shear, 1987) in conjunction with the low-pass filter were used to extract envelope information since carrier ITDs at high frequencies have little effect on lateralization (Henning, 1974). Further, the cutoff of 800 Hz was chosen because envelope rates above this value are also ineffective in lateralizing ITD-based binaural stimuli (Henning, 1974; Nuetzel and Hafter, 1981). The combination of the rectifier and low-pass filter were used instead of Hilbert-transform envelope extraction because of the nonlinear nature of the rectifier. This rectifier produces a more consistent fit with certain statistical predictions of binaural models for some noise stimuli (Colburn, 1969, 1977; Shear, 1987). The low-pass filter was followed by short-term cross correlation:

$$\Psi(t,f,\tau)=\frac{P(\tau)}{2T}\int_{-T}^{T}L(f,t)R(f,t-\tau)dt, \tag{11}$$

with a fixed time constant and an exponential center-weighting function, $P(\tau)$. This weighting function, which was the same as that used by Stern *et al.* (1988), scales the output of the cross correlator such that values near $\tau=0$ are more heavily weighted. The conventional exponential time decay (Sayers and Cherry, 1957; Blauert and Cobben, 1978) was omitted because it has no noticeable effect on this analysis.

Cross correlation was performed on $T=5$-ms samples of the waveform. This value is likely to be at the lowest extreme of an estimate for the time constant of cross correlation because envelope rates higher than about 100 Hz do not result in a difference in performance between comodulated and independent conditions. A noise bandwidth of 200 Hz (see Fig. 4) produces on the average, envelope peaks at a rate of 128 per second (Rice, 1944). We should also note that the sum of the short-term outputs is not considered here, although this sum may further contribute to predictions of improved thresholds for temporally coherent signals.

Figure 10 shows a representative output of this model for the complex SAM used in experiment II. The value shown next to each plot represents relative envelope-phase disparity (abscissa values in Fig. 7). When SAMs are in phase, two large peaks are evident. One peak progressively diminishes as the relative phase disparity between envelopes increases. Figure 11 shows that this predicted difference between phase conditions is reduced as the modulation rate increases. The output of the model is shown in this figure for an SAM complex identical to that used in experiment II except that the modulation rate was increased to 400 Hz. This output is nearly identical for the four phase conditions and therefore the detectability of ITDs for this signal is predicted to be largely independent of the relative envelope phase between the SAMs. The reduced cross-correlation activity at the lower frequency region for this latter stimulus may be explained by the output of single filters centered near the CFs of the SAMs. Figure 12 shows two such filters and their output for the complex SAM. The lower CF filter has steeper slopes and therefore the sidebands of the SAM in the lower CF filter are reduced in amplitude by a greater amount (by 6 to 9 dB) than the sidebands in the higher CF filter. The depth

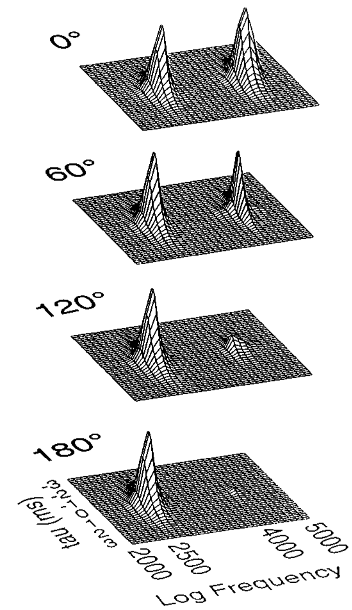

FIG. 10. The output of the model for the stimuli used in experiment II (SAM complex; modulation frequency of 50 Hz, carriers of 2.55 and 4.0 kHz). Each panel shows one phase condition (ITD=100 μs). The phase represents the relative starting phase between the two SAMs constituting the complex (Fig. 6).

of modulation, therefore, is less at the output of the lower CF filter which consequently produces a smaller peak at the cross-correlation output. The decrease in depth of modulation is more evident for the higher modulation rate for which the sidebands are widely spaced.

For comparison, we have also shown in Fig. 13 a representative output of this model for the noise bands used in experiment I. Left plots show the outputs for comodulated (upper plot) and independent (lower plot) 50-Hz-wide noise

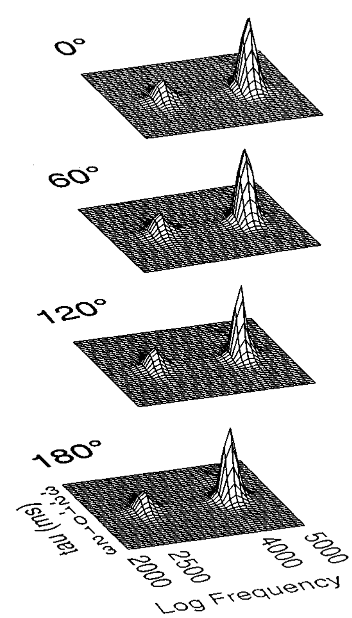

FIG. 11. The output of the model for an SAM complex consisting of two SAMs with a modulation rate of 400 Hz and carriers of 2.55 and 4.0 kHz (ITD=100 μs).

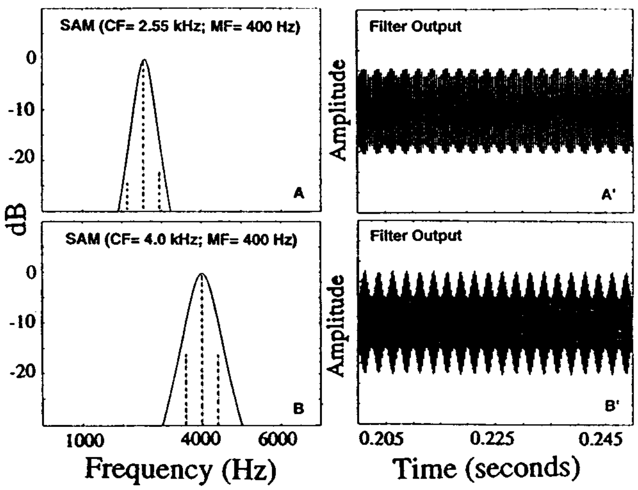

FIG. 12. Left panels show the spectrum of SAM signals with carriers and modulation frequencies shown within each panel. The filters, taken from the GammaTone filter bank, have CFs of 2573 and 3999 Hz. The slopes of the lower CF filter are sharper, hence the greater attenuation of the sidebands. The right panels show the output of each filter. The decreased depth of modulation for the lower CF signal results in less activity in the cross-correlation function at the lower frequency regions (Fig. 11).

bands. Two large peaks of activity are evident in the comodulated condition. For the 300-Hz-wide bands the output of the model is similar in the comodulated and independent conditions.

C. Within-channel cues

The edge of the spectrums of the narrow-band waveforms were, in the closest case, nearly two critical bands apart. Still, because the skirts of cochlear filters extend beyond critical bands, the manner in which the two waveforms interact within filters that are centered between them should be noted. If sufficient energy from each waveform leaks through a common filter, then the output of this filter will be more deeply modulated in the comodulated (or in-phase) condition, thus contributing to better performance in that case. Two points should be made about such cues. First, consider the noise band stimuli. The predictions of within-channel cues are contrary to the observed effects of bandwidth. The contribution of these cues should increase with bandwidth (largest at 300 Hz), while the data show a decrease of such a contribution with increasing bandwidth. Note that the higher modulation rate should not work against within-channel lateralization cues because rates of 200–300 Hz are optimum for lateralization of high-frequency complex stimuli. Second, consider the SAM waveforms. If we use the GammaTone filterbank for this analysis, the output of a filter centered halfway between the SAMs is 30 dB attenuated relative to on-frequency filters. This is only a modest attenuation; however, significant modulation-phase effects are still observed when signal SPL is 30 dB (inset to Fig. 7), and the within-channel cue has a level of 0 dB SPL in this case. Such near-absolute-threshold cues would have a negligible effect on lateralization, yet large phase-dependent effects are observed. Note also that the sidebands of the high- and low-carrier SAMs will be filtered asymmetrically; if, in addition, we consider that auditory filters introduce a relative phase shift between carrier and sidebands, it would then be unlikely that within-channel cues would follow the exact pattern of phase relations introduced by the waveforms or observed in the data. Still, a contribution from within-channels cues is not entirely discounted here. Another interesting explanation, the summed temporal envelope, should also be considered. This cue is different than within-channel interactions in that it is reported for waveforms separated by more than five octaves.

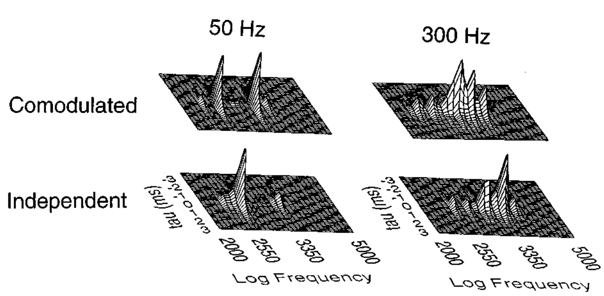

FIG. 13. Output of the model for the narrow-band noises of experiment I. The left plots show this output for 50-Hz-wide bands and the right plots for 300-Hz bands. The upper plots show the output for comodulated bands and the lower panels for statistically independent noise bands. Note that for the narrower bandwidth stimuli, the distinction between the comodulated and independent band conditions are more pronounced.

D. The summed temporal envelope

The summed temporal waveform of the complex noise has a greater peak-to-valley amplitude ratio when noise bands are comodulated compared to a complex consisting of independent noise bands. Similarly, the complex SAM tone has the greatest peak-to-valley amplitude ratio when the SAM envelopes are in phase (see Fig. 6). This ratio monotonically decreases as the envelope phase disparity increases. A discriminator which makes use of interaural delays carried by the overall temporal envelope of the complex will make a better estimate of ITDs when the SAMs are in phase because the overall depth of modulation will be greater (Henning, 1974; Nuetzel and Hafter, 1981). There is psychophysical evidence consistent with this view. Wakefield and Viemeister (1985) have shown that the detection of modulation in an SAM noise with a 10-kHz carrier depends on the phase of a simultaneously presented low-frequency tone (100, 200, or 400 Hz). This temporal interaction occurs when the frequency of the tone and the modulation frequency of the SAM noise are the same. Detection of modulation was reported to be best when the modulation phase of the SAM noise led that of the low-frequency tone by 90° and poorest when this phase difference was 270°. Surprisingly, these temporal interactions occurred in the absence of masking. The threshold for detection of the SAM noise was independent of the presence or absence of the low-frequency tone. Other psychophysical data are consistent with these ideas (Deatherage and Henderson, 1967; Zwicker, 1976, 1977; McFadden, 1975). Also consistent with this view, subjects in the current experiments reported the percept of a pulsating stimulus when the envelopes of the SAMs were homophasic, and a tonal signal when they were antiphasic. Evidence against this view includes the fact that Wakefield and Viemeister saw phase-dependent effects for modulation frequencies of 400 Hz, where phase dependence of performance for the complex SAMs in the current experiments is likely to be very small for this modulation frequency, as predicted from the noise data of experiment I. Second, the phase values for which they saw poorest and best performance do not match the pattern of changes in thresholds with phase shift observed in the current study.

ACKNOWLEDGMENTS

This research was supported by AFOSR and NIH. I thank Dr. Ervin R. Hafter, Dr. David M. Green, Dr. Constantine Trahiotis, Dr. Richard M. Stern, Dr. David A. Eddins, Dr. Raymond H. Dye, Jr., and two anonymous reviewers for helpful discussions.

[1]Although the waveforms at the two ears were gated simultaneously, because a phase-shift function was used to produce an interaural delay, each channel contained a brief portion of waveform that did not appear in the other channel. The duration of this difference in waveforms was equal to the duration of ITD and it appeared at the beginning and end of the waveforms. Because the maximum ITD was 0.6 ms and the signals were ramped with 10-ms functions, this difference in waveforms is negligible at its maximum (24 dB down; 0.003 proportion of waveform duration).

[2]It should be noted that the maximum ITD used in this experiment was 1200 μs (600 μs in each interval); the larger thresholds for the 50-Hz-bandwidth conditions were interpolations through the 75% point by fitting normal probability functions. This simply means that when a threshold of larger than 1200 μs is observed, the maximum ITD was, in fact, 1200 μs; however, subjects performed at less than 75% correct for this largest stimulus value presented (in general, for such cases observers performed at about 60% to 65%).

[3]The weighted-image model was originally proposed to estimate a position ($\hat{p}$) by appropriately weighting the contributions of straightness and centrality information. But one may make quantitative predictions regarding lateralization jnd's by estimating a variance ($\sigma^2_{\hat{p}}$) in addition to the expected value of this position variable; using optimal decision theory, statistically ideal discrimination may then be determined (van Trees, 1968; Green and Swets, 1966). For simplicity assume that $\sigma_{\hat{p}}$ is constant (Jeffress *et al.*, 1956; Hafter, 1971; Jeffress and McFadden, 1971). It should be clear that the greater the value of $\hat{p}$, the larger the estimated $d' = (\sqrt{2}\hat{p}/\sigma_{\hat{p}})$ in a 2IFC task. Now consider how $\hat{p}$ is affected by straightness [see Eqs. (2), (4), (5) of Stern *et al.*, 1988]. Equation (5) calculates a rms error about the ith trajectory. More straight trajectories produce a smaller σ_i^2 in Eq. (5). This means that the weight ω_i [Eq. (4)] will be larger since it is inversely proportional to σ_i^2. Consequently, $\hat{p}$ in Eq. (2) will be closer to μ_i, the real value of the "true" delay (straight trajectory). For smaller ω_i of the straight trajectory, $\hat{p}$ will be closer to zero. Thus given a constant variance d' will be larger when a measure of straightness additionally contributes to the position estimate $\hat{p}$. In extending this idea to high-frequency SAMs one should additionally assume a nonadditive (e.g., multiplicative) rule in combining straightness and centrality weights and a convention for determining cutoff frequencies in quantifying straightness weights for spectrally discontinuous waveforms.

Batteau, D. W. (**1967**). "The role of the pinna in human localization," Proc. R. Soc. London Ser. B **168**, 158–180.

Bernstein, L. R., and Trahiotis, C. (**1985**). "Lateralization of sinusoidally amplitude-modulated tones: Effects of spectral locus and temporal variation," J. Acoust. Soc. Am. **78**, 514–523.

Blauert, J., and Cobben, W. (**1978**). "Some consideration of binaural cross-correlation analysis," Acustica **39**, 96–104.

Buell, T. N., and Hafter, E. R. (**1991**). "Combination of binaural information across frequency bands," J. Acoust. Soc. Am. **90**, 1894–1900.

Buell, T. N., and Trahiotis, T. (**1993**). "Interaural temporal discrimination using two sinusoidally amplitude-modulated, high-frequency tones: Conditions of summation and interference," J. Acoust. Soc. Am. **93**, 480–487.

Buell, T. N., and Trahiotis, T. (**1994**). "Detection of interaural delay in bands of noise: Effects of spectral uncertainty and spectral interference," Assoc. Res. in Otolaryngol. Abstracts, p. 69.

Butler, R. A., and Belendiuk, K. (**1977**). "Spectral cues utilized in the localization of sound in the median saggital plane," J. Acoust. Soc. Am. **61**, 1264–1269.

Cohen, M. F., and Schubert, E. D. (**1987a**). "The effects of cross-spectrum correlation on the detectability of a noise band," J. Acoust. Soc. Am. **81**, 721–723.

Cohen, M. F., and Schubert, E. D. (**1987b**). "Influence of place synchrony on detection of a sinusoid," J. Acoust. Soc. Am. **81**, 452–458.

Cohen, M. F., and Schubert, E. D. (**1991**). "Comodulation masking release and the masking-level difference," J. Acoust. Soc. Am. **89**, 3007–3008.

Colburn, H. S. (**1969**). "Some Physiological Limitations on Binaural Performance," Ph.D. thesis, Department of Electrical Engineering, MIT.

Colburn, H. S. (**1977**). "Theory of binaural interaction based on auditory-nerve data. II. Detection of tones in noise." supplementary material, AIP Document No. PAPS JASMA-61-525-98, 1977, 61, 1–81.

Deatherage, B. H., and Henderson, D. (**1967**). "Auditory sensitization," J. Acoust. Soc. Am. **42**, 438–440.

Dye, R. H., and Hafter, E. R. (**1984**). "The effects of intensity on the detection of interaural differences of time in high-frequency trains of clicks," J. Acoust. Soc. Am. **75**, 1593–1598.

Dye, R. H. (**1990**). "The combination of interaural information across frequencies: Lateralization on the basis of interaural delay," J. Acoust. Soc. Am. **88**, 2159–2170.

Festen, J. M., and Plomp, R. (**1990**). "Effects of fluctuating noise and interfering speech on the speech-reception threshold for impaired and normal hearing," J. Acoust. Soc. Am. **88**, 1725–1736.

Green, D. M., and Swets, J. A. (**1966**). "*Signal Detection Theory and Psychophysics*" (Peninsula, Los Altos, CA), reprint, 1988.

Green, D. M., and Kidd, G., and Picardi, M. C. (**1983**). "Successive versus simultaneous comparison in auditory intensity discrimination," J. Acoust. Soc. Am. **73**, 639–643.

Green, D. M. (**1988**). *Profile Analysis* (Oxford U.P., Oxford).

Green, D. M., Dai, H., and Saberi, K. (**1995**). "Shape discrimination of spectra with various bandwidths," in *Advances in Hearing Research*, edited by G. A. Manley, G. M. Klump, C. Koppl, H. Fast, and H. Oeckinghaus (World Scientific, Singapore), pp. 501–511.

Grose, J. H., and Hall, J. W., III (**1992**). "Comodulation masking release for speech stimuli," J. Acoust. Soc. Am. **91**, 1042–1050.

Hafter, E. R. (**1971**). "Quantitative evaluation of a lateralization model of masking-level differences," J. Acoust. Soc. Am. **50**, 1116–1122.

Hall, J. W., III, Haggard, M. P., and Fernandes, M. A. (**1984**). "Detection in noise by spectro-temporal pattern analysis," J. Acoust. Soc. Am. **76**, 50–56.

Hall, J. W., III (**1986**). "The effect of across-frequency differences in masking level on spectro-temporal pattern analysis," J. Acoust. Soc. Am. **79**, 781–787.

Hall, J. W., III, and Haggard, M. P. (**1983**). "Co-modulation—A principle for auditory pattern analysis in speech," Int. Conf. Acoust. **11**, 69–71.

Hall, J. W., III, and Grose, J. H. (**1991**). "Masker envelope fluctuation and binaural masking release," *Auditory Physiology and Perception*, edited by Y. Cazals, L. Demany, and K. Horner (Pergamon, New York).

Heller, L. M., and Richards, V. M. (**1990**). "Lateral position and across-frequency envelope coherence," J. Acoust. Soc. Am. Suppl. 1 **87**, S63–S64.

Heller, L. M., and Trahiotis, C. (**1995**). "Interference in detection of interaural delay in a sinusoidally amplitude-modulated tone produced by a second, spectrally remote sinusoidally amplitude-modulated tone," J. Acoust. Soc. Am. **97**, 1808–1816.

Henning, G. B. (**1974**). "Detectability of interaural delay in high-frequency complex waveforms," J. Acoust. Soc. Am. **55**, 84–90.

Henning, G. B. (**1980**). "Some observations on the lateralization of complex waveforms," J. Acoust. Soc. Am. **68**, 446–453.

Henning, G. B., and Ashton, J. (**1981**). "The effect of carrier and modulation frequency on lateralization based on interaural phase and interaural group delay," Hear. Res. **4**, 185–194.

Holdsworth, J., Nimmo-Smith, I., Patterson, R., and Rice, P. (**1988**). "Implementing a GammaTone Filter Bank," Annex C of the SVOS final report (Part A: The auditory filter bank).

Houtgast, T., and van den Brink, W. A. C. (**1990**). ''Preferred spectrotemporal patterns in signal detection,'' J. Acoust. Soc. Am. Suppl. 1 **87**, S157.
Jeffress, L. A., Blodgett, H. C., Sandel, T. T., and Wodd, C. L., III (**1956**). ''Masking of tonal signals,'' J. Acoust. Soc. Am. **28**, 859–860.
Jeffress, L. A., and McFadden, D. M. (**1971**). ''Differences of interaural phase and level in detection and lateralization,'' J. Acoust. Soc. Am. **49**, 1169–1179.
Kuhn, G. F. (**1987**). ''Physical Acoustics and measurements pertaining to directional hearing,'' in *Directional Hearing*, edited by W. A. Yost and G. Gourevitch (Springer-Verlag, New York), pp. 3–25.
McFadden, D. (**1975**). ''Beat-like interaction between periodic waveforms,'' J. Acoust. Soc. Am. **57**, 983.
McFadden, D., and Pasanen, E. G. (**1976**). ''Lateralization at high frequencies based on interaural time differences,'' J. Acoust. Soc. Am. **59**, 634–639.
McFadden, D. (**1987**). ''Comodulation detection differences using noise-band signals,'' J. Acoust. Soc. Am. **81**, 1519–1527.
Moore, B. C. J. (**1990**). ''Co-modulation masking release: spectro-temporal pattern analysis in hearing,'' Br. J. Audiol. **24**, 131–137.
Nuetzel, J. M., and Hafter, E. R. (**1981**). ''Lateralization of complex waveforms: Spectral effects,'' J. Acoust. Soc. Am. **69**, 1112–1118.
Rice, S. O. (**1944**). ''Mathematical analysis of random noise,'' in *Selected Papers on Noise and Stochastic Processes*, edited by N. Wax (Dover, New York).
Richards, V. M. (**1987**). ''Monaural envelope correlation perception,'' J. Acoust. Soc. Am. **82**, 1621–1630.
Sayers, B. McA., and Cherry, E. C. (**1957**). ''Mechanism of binaural fusion in hearing of speech,'' J. Acoust. Soc. Am. **29**, 973–987.
Schooneveldt, G. P., and Moore, B. C. J. (**1989**). ''Comodulation masking release (CMR) as a function of masker bandwidth, modulator bandwidth and signal duration,'' J. Acoust. Soc. Am. **85**, 273–281.
Shaw, E. A. G. (**1979**). ''External ear response and sound localization,'' in *Localization of Sound: Theory and Applications*, edited by R. W. Gatehouse (Amphora, Groton, CT).
Shear, G. D. (**1987**). ''Modeling the Dependence of Auditory Lateralization on Frequency and Bandwidth,'' Master thesis, Department of Electrical Engineering, Carnegie Mellon University.
Spiegel, M. F., and Green, D. M. (**1982**). ''Signal and masker uncertainty with noise maskers of varying duration bandwidth, and center frequency,'' J. Acoust. Soc. Am. **71**, 1204–1210.
Stellmack, M. A., and Dye, R. H. (**1993**). ''The combination of interaural information across frequencies: The effects of number and spacing of components, onset asynchrony, and harmonicity,'' J. Acoust. Soc. Am. **93**, 2933–2947.
Stellmack, M. A. (**1992**). ''Detection of an interaural delay of a reproducible target noise band in the presence of reproducible diotic noise bands,'' J. Acoust. Soc. Am. **92**, 2363.
Stern, R. M., Zeiberg, A. S., and Trahiotis, C. (**1988**). ''Lateralization of complex binaural stimuli: a weighted-image model,'' J. Acoust. Soc. Am. **84**, 156–165.
Takahashi, T. A., and Konishi, M. (**1986**). ''Selectivity for interaural time differences in the Owl's midbrain,'' J. Neurosci. **6**, 3413–3422.
Trahiotis, T., and Bernstein, L. R. (**1990**). ''Detectability of interaural delays over select spectral regions: Effects of flanking noise,'' J. Acoust. Soc. Am. **87**, 810–813.
Trahiotis, T., and Stern, R. M. (**1994**). ''Across-frequency interaction in lateralization of complex binaural stimuli,'' J. Acoust. Soc. Am. **96**, 3804–3806.
van Trees, H. L. (**1968**). *Detection Estimation, and Modulation Theory*, Part I (Wiley, New York).
Wakefield, G. H., and Viemeister, N. F. (**1985**). ''Temporal interactions between pure tones and amplitude-modulated noise,'' J. Acoust. Soc. Am. **77**, 1535–1542.
Yost, W. A., and Sheft, S. (**1989**). ''Across-critical-band processing of amplitude-modulated tones,'' J. Acoust. Soc. Am. **85**, 848–857.
Zurek, P. M. (**1985**). ''Spectral dominance in sensitivity to interaural delay for broadband stimuli,'' J. Acoust. Soc. Am. Suppl. 1 **78**, S18.
Zwicker, E. (**1976**). ''Psychoacoustic equivalent of period histograms,'' J. Acoust. Soc. Am. **59**, 166–175.
Zwicker, E. (**1977**). ''Masking-period patterns produced by very-low-frequency maskers and their possible relation to basilar-membrane displacement,'' J. Acoust. Soc. Am. **61**, 1031–1040.